



Proceeding Paper

# Molecular Docking and Dynamics of a Series of Aza-Heterocyclic Compounds Against Effector Protein NleL <sup>+</sup>

Karen Astrid Ortiz-Vargas <sup>1</sup>, Juan Pedro Palomares-Báez <sup>2</sup>, Judit A. Aviña-Verduzco <sup>1</sup>, Hugo A. García-Gutiérrez <sup>1</sup>, Rafael Herrera-Bucio <sup>1</sup> and Pedro Navarro-Santos <sup>3,\*</sup>

- <sup>1</sup> Instituto de Investigaciones Químico Biológicas, Universidad Michoacana de San Nicolás de Hidalgo, Morelia 58030, Mexico; 1718959h@umich.mx (K.A.O.-V.); jaavina@umich.mx (J.A.A.-V.); hgarcia@umich.mx (H.A.G.-G.); rafael.herrera.bucio@umich.mx (R.H.-B.).
- <sup>2</sup> Facultad de Ciencias Químicas, Universidad Autónoma de Chihuahua, Chihuahua 31125, Mexico; ppalomares@uach.mx
- <sup>3</sup> SECIHTI-Instituto de Investigaciones Químico Biológicas, Universidad Michoacana de San Nicolás de Hidalgo, Morelia 58030, Mexico
- \* Correspondence: pedro.navarro@umich.mx; Tel.: +52-443-2239793
- <sup>†</sup> Presented at the 29th International Electronic Conference on Synthetic Organic Chemistry (ECSOC-29); Available online: https://sciforum.net/event/ecsoc-29.

#### **Abstract**

The Shiga toxin-producing strain of *Escherichia coli* with serotype O157:H7 can cause acute bloody diarrhea, which can lead to life-threatening hemolytic uremic syndrome. According to the World Health Organization, this bacterium causes 2.8 million cases annually. Therefore, this theoretical study based on molecular docking and dynamics examined the inhibitory capacity of a series of aza-heterocyclic derivatives against the effector protein NleL of enterohemorrhagic *E. coli* (PDB ID: 3NAW), by determining affinity energy, stability, H-bond interactions and binding free energies of the compounds. The results obtained have enabled the identification of compounds with the potential to inhibit this infectious strain, contributing to an understanding of this protein.

**Keywords:** molecular docking; molecular dynamics; binding free energy; effector protein NleL; aza-heterocyclic compounds

Academic Editor(s): Name

Published: date

Citation: Ortiz-Vargas, K.A.;
Palomares-Báez, J.P.; AviñaVerduzco, J.A.; García-Gutiérrez,
H.A.; Herrera-Bucio, R.;
Navarro-Santos, P. Molecular
Docking and Dynamics of a Series of
Aza-Heterocyclic Compounds
Against Effector Protein NleL. Chem.
Proc. 2025, volume number, x.
https://doi.org/10.3390/xxxxx

Copyright: © 2025 by the authors. Submitted for possible open access publication under the terms and conditions of the Creative Commons Attribution (CC BY) license (https://creativecommons.org/license s/by/4.0/).

# 1. Introduction

The Gram-negative bacterium *Escherichia coli*, commonly found in the human intestine, is typically harmless. However, the Shiga toxin-producing strain with serotype O157:H7 is primarily transmitted through the consumption of contaminated food such as raw or undercooked meat, raw or poorly pasteurized milk, and fruits and vegetables contaminated with feces from an infected animal [1,2]. The symptoms of the infection usually include fever, vomiting, abdominal cramps, and diarrhea, which can progress to bloody diarrhea (hemorrhagic colitis) [2]. The disease lasts about ten days; nonetheless, the infection can lead to hemolytic uremic syndrome, especially in young children and the elderly, with a fatality rate of 3 to 5% [2].

To combat serotype O157:H7, only intravenous fluids are usually administered because the use of antibiotics, such as fluoroquinolones, is considered to increase the release of enterotoxins, increasing diarrhea and the possibility of developing hemolytic uremic syndrome [1].

Chem. Proc. 2025, x, x https://doi.org/10.3390/xxxxx

Lin, D. Y. W. et al. [3] characterized the non-Lee-encoded effector ligase (NleL) from enterohemorrhagic *E. coli* O157:H7 (PDB ID: 3NAW), which mimics the structure and function of eukaryotic HECT E3 ligases, playing vital roles in bacterial adhesion, entry, and survival and modulating host cellular functions such as cytoskeletal dynamics, gene expression, and post-translational modification. NleL also catalyzes the formation of unanchored polyubiquitin chains by forming specific bonds with the Lys6 and Lys48 sites of the ubiquitin, as well as with its own catalytic Cys753 residue which, forms a thioester intermediate with ubiquitin, thereby regulating the process [3]. The final amino acid in this sequence is known to be essential for the activity of the E3 ligase [3]. Interactions between NleL and the E2 enzyme have been found. These interactions include important van der Waals interactions with Phe569 of NleL as well as interactions, near the catalytic amino acid, with the polar residues Glu705, Tyr706, and Asp707 [4]. Finally, there are interactions of Asn578 of the NleL protein and Phe63 of E2, which are responsible for most of the contacts between them [5]. Additionally, hydrophobic interactions with the E2 enzyme and E3 ligases are critical for molecular recognition [4].

Although knowledge about the functions of pentapeptide repeat proteins is limited, it is known that E3 ubiquitin ligases can act simply as a scaffold to provide the surface area required to support binding interactions with another protein [5]. Elucidating the function of these proteins may contribute to a deeper comprehension of the pathogenesis of this bacterium.

# 2. Materials and Methods

# 2.1. Molecular Docking

The structures of the proposed compounds [6,7] shown in Figure 1 were retrieved from PubChem [8] (specifically ligands 1, 2, 4, and 5) or were built in Spartan [9] (ligands 3, 6, 7, and 8). Then, the ligands were prepared by adding all their hydrogen atoms and detecting their rotatable bonds using Discovery Studio [10] and AutoDockTools [11], respectively. The effector protein NleL was obtained from the RCSB PDB [12] (PDB ID: 3NAW) with a resolution = 2.5 Å and was isolated in Chimera [13]. Subsequently, the receptor was prepared by adding all its hydrogen atoms, merging the non-polar ones, and adding the Kollman charges with AutoDockTools. Thereafter, AutoDock GR was employed to identify the potential inhibition sites.

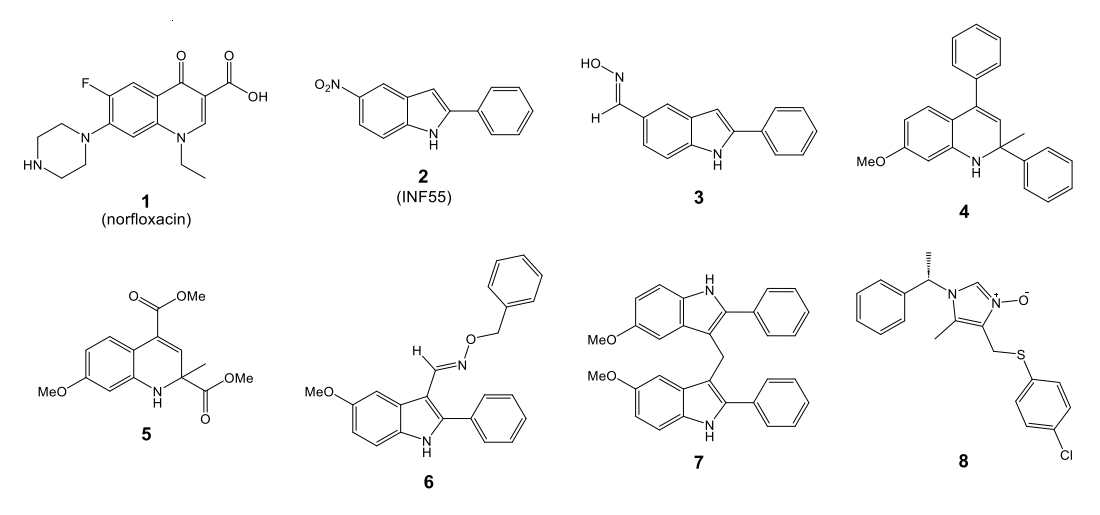


**Figure 1.** Molecular structure of the aza-heterocyclic compounds analogous to INF55 proposed as inhibitors of the effector protein NleL.

In the molecular docking process, approximately 5 amino acids were selected to allow flexibility within each site, with a padding of 4 Å, employing the AutoDock FR software package [14,15], and considering a seed number of 1, which refers to the random number generator seed used to initialize the stochastic search algorithms and allows for a docking calculation to be reproduced for a given version of the code.

Subsequently, the best conformation of each ligand at each site was selected, and the best site was chosen according to its proximity to the amino acids of interest, as described in the literature.

# 2.2. Molecular Dynamics

The best conformation of each ligand for the selected inhibition site in the receptor was evaluated employing molecular dynamics simulations. First, the ligand was prepared by adding its hydrogens at pH = 7.4 using Avogadro [16] and was parametrized with the "Ligand Reader & Modeler" module of the CHARMM-GUI server [17,18]. Then, the complex between each parametrized ligand and the receptor was formed in Chimera. In the "Solution Builder" module of CHARMM-GUI, the complex was prepared at a pH = 7.4, in a rectangular cell of  $138 \times 138 \times 138 \times 138$  ų, solvated with a TIP3P water model [19] and neutralized by adding NaCl ions at 0.15 M with the Monte Carlo method to collocate these ions. The force field used for the simulations was CHARMM36m [20] and long-range electrostatic interactions were modeled with the particle mesh Ewald (PME) method [21] and a 12 Å cutoff for non-bonded interactions.

The molecular dynamics simulations were performed in four stages using the software NAMD [22]. First, an energy minimization was done using a conjugate gradient algorithm [23] with 100,000 iteration steps and a time step of 1.0 fs. Second, the NVT ensemble was performed to heat from 0 to 310 K at 1 K intervals for a period of 500 ps, and then the temperature was maintained at 310 K for an additional 500 ps using the Langevin thermostat. Third, an equilibration was performed by means of the NPT ensemble at 1 atm and 310 K for a period of 2.5 ns with a time step of 1 fs using the Langevin thermostat and the Nosé-Hoover Langevin piston barostat [24,25]. Fourthly, production was executed with the NPT ensemble for a duration of 50 ns, with a time step of 2 fs. To ensure the energy stabilization of the most promising complexes, the simulation was extended to 100 ns.

From the production stage of the molecular dynamics simulations, the root mean square deviation (RMSD) values of the protein backbone and the ligand aligned to the protein were determined to evaluate the stability of the complexes and the residence of the hydrogen bond interactions, considering the maximum donor-acceptor distance of 3.2 Å and a cutoff angle of 50° using VMD [26]. Then, the properties and the binding free energies were calculated using the molecular mechanics-generalized Born surface area (MM/GBSA) model with the gmx\_MMPBSA tool [27] for the final 50 ns, exploring an average of 500 snapshots.

# 3. Results

#### 3.1. Molecular Docking

The affinity energies determined from the molecular docking assessments for the selected inhibition site are shown in Table 1, and the interaction maps of each ligand against the receptor are shown in Figure S1. (See Figure S1 from the Supplementary Materials).

Table 1. Affinity energies (in kcal/mol) for the ligands 1–8 against the receptor effector protein NleL.

Ligand	Affinity Energies
1	-7.2

2	-7.4
3	-8.2
4	-9.3
5	-7.7
6	-9.0
7	-9.1
8	-8.3

# 3.2. Molecular Dynamics

The RMSD values for the protein backbone (Figure 2a) and the ligand aligned to the protein (Figure 2b), of the most stable complexes studied in this work, are shown in Figure 2, and they can be represented in quantitative terms in Table S1. (See Table S1 from the Supplementary Materials).

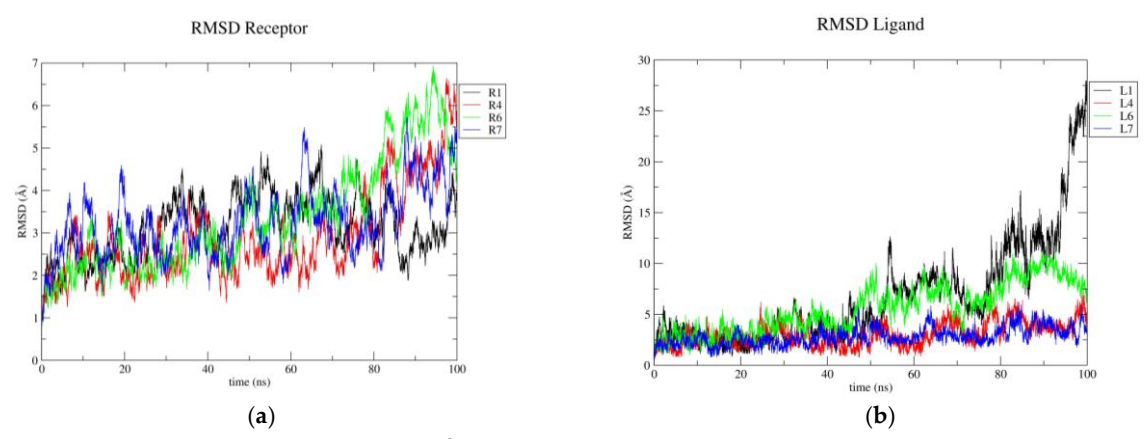


**Figure 2.** RMSD (in Å) (**a**) of the receptor and (**b**) of the ligand aligned to the receptor in each complex.

Regarding the hydrogen bond interactions between the ligands and the receptor during the 100 ns, those with a percentage greater than 5% are shown in Table 2.

Ligand	Donor	Acceptor	% of Occupancy
1	GLN605	LIG	8.60
4	LIG	SER604	54.46
6	LIG	LEU775	43.08
	LIG	SER604	43.14
	VAL779	LIG	6.06
7	VAL608	LIG	29.60
	LIG	LEU775	38.58
	LIG	ASN630	37.40

**Table 2.** H-bond interactions observed during the 100 ns of simulation.

For the simulated ligands for 100 ns, the binding free energy was subsequently determined using MMGBSA, calculating only the free energy during the last 50 ns and obtaining the results shown in Table 3.

**Table 3.** The predicted binding free energies (in kcal/mol) of the ligands against the effector protein NleL, obtained using the MMGBSA method.

Ligand	$\Delta G$ van der Waals	$\Delta G$ Electrostatic	<b>Binding Free Energies</b>
1	-16.09	-7.48	-8.20
4	-28.44	-7.14	-20.58
6	-41.18	-20.79	-32.57

7 -37.26 -13.81 -23.80

# 4. Discussion

# 4.1. Molecular Docking

Table 1 shows that for the selected binding site, the ligand with the best affinity energy was 4, followed by ligands 7 and 6, all of which have values better than or equal to –9 kcal/mol. According to Figure S1, all the ligands exhibited many interactions. Ligand 5 has the greatest number of interactions, followed by ligands 6 and 7, all these exhibit only favorable interactions. However, ligands 1 and 4 exhibit the same number of favorable interactions as ligand 7 but additionally exhibit unfavorable interactions. All the ligands exhibit at least one favorable interaction with Leu775, seven of the ligands exhibit favorable interactions with Lys601, Val608, and Pro778, and five of the ligands exhibit interactions with Ser604, Leu629, and Arg782.

#### 4.2. Molecular Dynamics

According to Figure 2a and Table S1, the receptor demonstrates enhanced stability in the presence of ligand 1, compared to its response to the other ligands. In general, the receptor in the presence of the ligands has average RMSD values in the range of 2.9 to 3.3 Å. Figure 2b shows that ligands 4, 6, and 7 remain in the analyzed region, while ligand 1 diffuses to another region of the protein. Based on Table S1, ligands 7 and 4, have the lowest average RMSD values, at 2.8 and 3.1 Å, respectively.

As indicated by the data presented in Table 2, the highest number of interactions greater than 5% was observed for ligands 6 and 7. However, only ligand 4 exhibits an interaction greater than 50% with Ser604. Ligand 6 also exhibits an interaction with Ser604 with an occupancy percentage slightly below 50%.

Table 3 shows that ligand 6 exhibits the lowest binding free energy indicating the highest affinity for the 3NAW target. On the other hand, ligands 4 and 7 exhibit similar but higher free energies than ligand 6. Meanwhile, ligand 1 has a much higher binding free energy, probably because it diffused to another region of the receptor and failed to stabilize. Besides, the van der Waals interactions were found to contribute more to the binding free energy in all cases, which represents that hydrophobic interactions play an important role in helping to stabilize the ligands in the complex.

## 5. Conclusions

According to the analysis of molecular docking assessments, potential inhibition sites were identified; however, none were found in the catalytic amino acid Cys753. In contrast, inhibition site 1 was found near this amino acid. Consequently, the inhibition site 1 was selected for further investigation through molecular dynamics simulations.

For the molecular docking assessments in the selected inhibition site, the ligands exhibiting higher affinity and more favorable interactions were 4, 6, and 7. Subsequent molecular dynamics simulations, revealed that the ligands 4, 6, and 7 remained in the inhibition site during the simulation and exhibited substantial stability and hydrogen bond interactions. Nevertheless, ligand 6 demonstrated the optimal binding free energy, exhibiting a considerable difference from the binding free energies of ligands 4 and 7. It can be concluded that the interactions that most contribute to the binding free energy are van der Waals for the most promising ligands. However, amino acids Ser604 and Leu775 have been shown to play a vital role in the stabilization of ligands through the formation of hydrogen bonds. Considering these findings, it is thought that the molecular structure of ligand 6 could serve as a guide in the development of potential inhibitors of this enzyme and could help to understand the importance of this protein in bacterial survival.

**Supplementary Materials:** The following supporting information can be downloaded at: https://www.mdpi.com/article/doi/s1, Figure S1. Interactions and distances (in Å) for ligands (a) 1, (b) 2, (c) 3, (d) 4, (e) 5, (f) 6, (g) 7, and (h) 8 against the effector protein NleL.; Table S1. Average and maximum RMSD (in Å) (a) of the receptor and (b) of the ligand aligned to the receptor for the 100 ns.

**Author Contributions:** Conceptualization, software, writing—review and editing, project administration, R.H.-B. and P.N.-S.; methodology, visualization, K.A.O.-V., R.H.-B. and P.N.-S.; validation, K.A.O.-V. and H.A.G.-G.; formal analysis, K.A.O.-V. and J.P.P.-B.; resources, P.N.-S.; data curation, K.A.O.-V. and J.A.A.-V.; writing—original draft preparation, investigation, K.A.O.-V.; supervision, J.P.P.-B., J.A.A.-V., H.A.G.-G., R.H.-B. and P.N.-S. All authors have read and agreed to the published version of the manuscript.

Funding: This research received no external funding.

Institutional Review Board Statement: Not applicable.

**Informed Consent Statement:** Not applicable.

**Data Availability Statement:** The original contributions presented in this study are included in the article/Supplementary Materials. Further inquiries can be addressed to the corresponding author upon request.

**Acknowledgments:** This work was supported by the Secretaría de Ciencia, Humanidades, Tecnología e Innovación (Secihti) and Universidad Michoacana de San Nicolás de Hidalgo. P.N.-S. gives thanks to Secihti for infrastructure grant No. 262232, and K.A.O.-V. gives thanks to Secihti for Ph. D. scholarship number 1267478.

Conflicts of Interest: The authors declare no conflicts of interest.

# References

- Bush, L.M. Infecciones por Escherichia coli. Available online: https://www.msdmanuals.com/es/hogar/infecciones/infecciones-bacterianas-bacterian-gramnegativas/infecciones-por-escherichia-coli (accessed on 10 September 2025).
- 2. World Health Organization. *E. coli*. Available online: https://www.who.int/es/news-room/fact-sheets/detail/e-coli (accessed on 10 September 2025).
- 3. Lin, D.Y.W.; Diao, J.; Zhou, D.; Chen, J. Biochemical and Structural Studies of a HECT-like Ubiquitin Ligase from *Escherichia coli* O157:H7. *J. Biol. Chem.* **2011**, 286, 441–449. https://doi.org/10.1074/jbc.m110.167643.
- 4. Lin, D.Y.W.; Diao, J.; Chen, J. Crystal structures of two bacterial HECT-like E3 ligases in complex with a human E2 reveal atomic details of pathogen-host interactions. *Proc. Natl. Acad. Sci. USA* **2012**, *109*, 1925–1930. https://doi.org/10.1073/pnas.1115025109.
- 5. Zhang, R.; Kennedy, M.A. Current Understanding of the Structure and Function of Pentapeptide Repeat Proteins. *Biomolecules* **2021**, *11*, 638. https://doi.org/10.3390/biom11050638.
- Gutiérrez, R.U.; Correa, H.C.; Bautista, R.; Vargas, J.L.; Jerezano, A.V.; Delgado, F.; Tamariz, J. Regioselective Synthesis of 1,2-Dihydroquinolines by a Solvent-Free MgBr2-Catalyzed Multicomponent Reaction. J. Org. Chem. 2013, 78, 9614–9626. https://doi.org/10.1021/jo400973g.
- Gutiérrez, R.U.; Rebollar, A.; Bautista, R.; Pelayo, V.; Várgas, J.L.; Montenegro, M.M.; Espinoza-Hicks, C.; Ayala, F.; Bernal, P.M.; Carrasco, C.; et al. Functionalized α-oximinoketones as building blocks for the construction of imidazoline-based potential chiral auxiliaries. *Tetrahedron Asymmetry* 2015, 26, 230–246. https://doi.org/10.1016/j.tetasy.2015.01.011.
- 8. Kim, S.; Chen, J.; Cheng, T.; Gindulyte, A.; He, J.; He, S.; Li, Q.; Shoemaker, B.; Thiessen, P.; Yu, B.; et al. PubChem 2025 update. *Nucleic Acids Res.* **2025**, *53*, D1516–D1525. https://doi.org/10.1093/nar/gkae1059.
- 9. Wavefunction\_Inc. Spartan'20 (Version 20.1.3); Q-CHEM: Pleasanton, CA, USA, 2020.
- 10. BIOVIA. Dassault Systèmes BIOVIA, Discovery Studio Modeling Environment, 2019; Dassault Systèmes: San Diego, CA, USA, 2019.
- Morris, G.M.; Huey, R.; Lindstrom, W.; Sanner, M.F.; Belew, R.K.; Goodsell, D.S.; Olson, A.J. Autodock4 and AutoDockTools4: Automated docking with selective receptor flexibility. J. Comput. Chem. 2009, 16, 2785–2791. https://doi.org/10.1002/jcc.21256.
- 12. Berman, H.M.; Westbrook, J.; Feng, Z.; Gilliland, G.; Bhat, T.N.; Weissig, H.; Shindyalov, I.N.; Bourne, P.E. The Protein Data Bank. *Nucleic Acids Res.* **2000**, *28*, 235–242. https://doi.org/10.1093/nar/28.1.235.

- 13. Pettersen, E.F.; Goddard, T.D.; Huang, C.C.; Couch, G.S.; Greenblatt, D.M.; Meng, E.C.; Ferrin, T.E. UCSF Chimera—A visualization system for exploratory research and analysis. *J. Comput. Chem.* **2004**, *25*, 1605–1612. https://doi.org/10.1002/jcc.20084.
- 14. Sanner, M.F. AutoDockFR Home Page. Available online: https://ccsb.scripps.edu/adfr/ (accessed on 10 September 2025).
- 15. Ravindranath, P.A.; Forli, S.; Goodsell, D.S.; Olson, A.J.; Sanner, M.F. AutoDockFR: Advances in Protein-Ligand Docking with Explicitly Specified Binding Site Flexibility. *PLoS Comput. Biol.* **2015**, *11*, e1004586. https://doi.org/10.1371/journal.pcbi.1004586.
- 16. Hanwell, M.D.; Curtis, D.E.; Lonie, D.C.; Vandermeersch, T.; Zurek, E.; Hutchison, G.R. Avogadro: An advanced semantic chemical editor, visualization, and analysis platform. *J. Cheminform.* **2012**, *4*, 17. https://doi.org/10.1186/1758-2946-4-17.
- 17. Kim, S.; Lee, J.; Jo, S.; Brooks III, C.L.; Lee, H.S.; Im, W. CHARMM-GUI ligand reader and modeler for CHARMM force field generation of small molecules. *J. Comput. Chem.* **2017**, *38*, 1879–1886. https://doi.org/10.1002/jcc.24829.
- 18. Jo, S.; Kim, T.; Iyer, V.G.; Im, W. CHARMM-GUI: A web-based graphical user interface for CHARMM. *J. Comput. Chem.* **2008**, 29, 1859–1865. https://doi.org/10.1002/jcc.20945.
- 19. Jorgensen, W.L.; Chandrasekhar, J.; Madura, J.D.; Impey, R.W.; Klein, M.L. Comparison of simple potential functions for simulating liquid water. *J. Chem. Phys.* **1983**, *79*, 926–935. https://doi.org/10.1063/1.445869.
- 20. Huang, J.; Rauscher, S.; Nawrocki, G.; Ran, T.; Feig, M.; de Groot, B.L.; Grubmüller, H.; MacKerell, A.D. CHARMM36m: An improved force field for folded and intrinsically disordered proteins. *Nat. Methods* **2017**, *14*, 71–73. https://doi.org/10.1038/nmeth.4067.
- 21. Essmann, U.; Perera, L.; Berkowitz, M.L.; Darden, T.; Lee, H.; Pedersen, L.G. A smooth particle mesh Ewald method. *J. Chem. Phys.* **1995**, *103*, 8577–8593. https://doi.org/10.1063/1.470117.
- 22. Phillips, J.C.; Hardy, D.J.; Maia, J.D.C.; Stone, J.E.; Ribeiro, J.V.; Bernardi, R.C.; Buch, R.; Fiorin, G.; Hénin, J.; Jiang, W.; et al. Scalable molecular dynamics on CPU and GPU architectures with NAMD. *J. Chem. Phys.* **2020**, *153*, 044130. https://doi.org/10.1063/5.0014475.
- 23. Fletcher, R.; Reeves, C.M. Function minimization by conjugate gradients. *Comput. J.* **1964**, 7, 149–154. https://doi.org/10.1093/comjnl/7.2.149.
- 24. Martyna, G.J.; Tobias, D.J.; Klein, M.L. Constant pressure molecular dynamics algorithms. *J. Chem. Phys.* **1994**, *101*, 4177–4189. https://doi.org/10.1063/1.467468.
- 25. Feller, S.E.; Zhang, Y.; Pastor, R.W.; Brooks, B.R. Constant pressure molecular dynamics simulation: The Langevin piston method. *J. Chem. Phys.* **1995**, *103*, 4613–4621. https://doi.org/10.1063/1.470648.
- 26. Humphrey, W.; Dalke, A.; Schulten, K. VMD—Visual Molecular Dynamics. *J. Mol. Graph.* **1996**, *14*, 33–38. https://doi.org/10.1016/0263-7855(96)00018-5.
- 27. Valdés-Tresanco, M.S.; Valdés-Tresanco, M.E.; Valiente, P.A.; Moreno, E. gmx\_MMPBSA: A New Tool to Perform End-State Free Energy Calculations with GROMACS. *J. Chem. Theory Comput.* **2021**, 17, 6281–6291. https://doi.org/10.1021/acs.jctc.1c00645.

**Disclaimer/Publisher's Note:** The statements, opinions and data contained in all publications are solely those of the individual author(s) and contributor(s) and not of MDPI and/or the editor(s). MDPI and/or the editor(s) disclaim responsibility for any injury to people or property resulting from any ideas, methods, instructions or products referred to in the content.